Sympathetic Cooling of $^4He^+$ Ions in a Radio-Frequency Trap

B. Roth, U. Fröhlich, and S. Schiller

Institut für Experimentalphysik, Heinrich–Heine–Universität Düsseldorf, 40225 Düsseldorf, Germany

(Received 23 July 2004; published 7 February 2005)

We have generated Coulomb crystals of ultracold $^4He^+$ ions in a linear radio-frequency trap, by sympathetic cooling via laser-cooled $^9Be^+$. Stable crystals containing up to 150 localized He^+ ions at $\sim$20 mK were obtained. Ensembles or single ultracold He^+ ions open up interesting perspectives for performing precision tests of QED and measurements of nuclear radii. This Letter also indicates the feasibility of cooling and crystallizing highly charged atomic ions using $^9Be^+$ as coolant.

DOI: 10.1103/PhysRevLett.94.053001 PACS numbers: 32.80.Pj, 42.50.−p

The two-body Coulomb system is one of the most fundamental in physics, and has been central in the development of quantum mechanics, relativistic quantum mechanics, and QED. In nuclear physics, the study of these systems can provide an alternative method for precise determination of nuclear sizes [1]. Hydrogenlike systems studied include the hydrogen atom and its isotopes, muonic hydrogen, the helium ions, muonium, and positronium. More recently, heavy (high-Z) hydrogenlike ions have become available [2] and are being used, e.g., for exploring strong-field QED [3] and for measuring the electron mass [4]. Among the low-Z atomic systems, hydrogen has been the most extensively studied, in particular, by laser spectroscopy. This has resulted, among others, in the most precise measurement of a fundamental constant, the Rydberg constant [5]. While the helium ions $^3He^+$ and $^4He^+$ are important systems because they are complementary to the hydrogen atom, they have been much less studied. Precision measurements of transition frequencies in He^+ ions could provide (i) an independent (metrologically significant) determination of the Rydberg constant, (ii) an independent determination of the nuclear charge radii and the isotope shift, assuming QED (Lamb shift) calculations are correct, or (iii) a test of QED, using independent radius data (from scattering measurements) as input.

Precise values of the He nuclear radii can test theoretical nuclear methods and force models, which accurately describe these special nuclei (^3He is the only stable three-particle nucleus, ^4He is the lightest closed-shell nucleus). The possibility of QED tests with He ions is attractive because the QED corrections scale with high powers of Z (some of the theoretically unknown contributions scale as Z^6), and thus their relative contribution to transition frequencies is larger than in hydrogen. Also, the available independent $^4He^+$ nuclear radius measurements agree, in contrast to the situation in hydrogen.

On the experimental side, the hyperfine structure of $^3He^+$ has been measured in both the electronic $1S$ ground state and the $2S$ excited state [6]. The Lamb shift of the $2S$ state in $^4He^+$ has been determined from the spontaneous emission anisotropy with 170 kHz uncertainty and compared to theoretical calculations [7,8]. The $^3He/^4He$ squared nuclear radius difference has been determined at the 0.4% level from the isotope shift in neutral helium using laser spectroscopy [9].

A significant extension of these studies would be accessible via high-resolution laser spectroscopy of helium ions, which has not been performed so far. Measurements of the $1S$-$2S$ and $2S$-$3S$ two-photon transition frequencies (at 61 and 328 nm, with linewidths 167 Hz and 16 MHz, respectively) have been proposed [10,11]. For example, a $1S$-$2S$ measurement with reasonable experimental uncertainty $<$30 kHz would test the nuclear and the recently improved theoretical QED contributions at their current accuracy level [12]. A measurement of the isotope shift with a similar accuracy would improve the value of the squared nuclear charge radius difference by an order of magnitude.

One important aspect in these future precision experiments will be the availability of trapped ultracold helium ions, in order to minimize the influence of Doppler broadening or shifts and to allow a precise study of systematic effects. The experience with trapped ions for atomic clocks has shown the success of this approach [13].

In this Letter we report on the first production of an ultracold sample of $^4He^+$. While trapping of these ions is straightforward using a Paul-type trap [14], cooling is more difficult. Direct laser cooling appears impractical at present, since the generation of the required continuous-wave deep-UV 30 nm radiation is a challenging problem in itself. An alternative and flexible method is sympathetic (interaction) cooling, where ''sample'' particles of one species are cooled by an ensemble of directly cooled (often by laser cooling) particles of another species via their mutual interaction. This method was first demonstrated for ions in Penning traps [15,16], and later in Paul traps [17–19]. Under strong cooling, the mixed-species ensemble forms a Coulomb crystal. In sympathetic crystallization of large ensembles a minimum mass ratio range m_{sc}/m_{lc} of 0.6 between sympathetically cooled and laser-cooled ions has so far been achieved [20]. Recent molecular dynamics simulations showed that sympathetic cooling

in an ion trap down to a mass ratio of 0.3 should be possible [21,22]. A two-ion sympathetically cooled crystal exhibited a mass ratio of 0.38 [23]. In the present work we have used the lightest atomic ion suitable for practical laser cooling, $^9Be^+$, for which the mass ratio to $^4He^+$ is 0.44.

We use a linear quadrupole trap to simultaneously store Be^+ and He^+ ions. It consists of four cylindrical electrodes, each sectioned longitudinally into three parts. A necessary condition for stable trapping is a stability parameter, $q = 2QV_{\rm rf}/m\Omega^2 r_0^2 < 0.9$. Here, Q and m are the charge and the mass of the trapped ions, $V_{\rm rf}$ and Ω are the amplitude and the frequency of the rf driving field and $r_0 = 4.3$ mm is the distance from the trap centerline to the electrodes. Trap operation at small q parameters is favorable since rf-heating effects are less pronounced. We operate our trap at $\Omega = 2\pi \times 14.2$ MHz and $V_{\rm rf} = 380$ V where $q \simeq 0.04$ (0.1) for Be^+ (He^+). For such small q one can approximate the motion of ions (in the absence of interactions) by that in an effective time-independent harmonic potential $U_{\rm trap}(x, y, z) = \frac{m}{2}[\omega_r^2(x^2 + y^2) + \omega_z^2 z^2]$. The z axis is along the trap centerline. Oscillations transverse to the z axis occur with frequency $\omega_r = (\omega_0^2 - \omega_z^2/2)^{1/2}$, with $\omega_0 = QV_{\rm rf}/\sqrt{2}m\Omega r_0^2$ being the limiting value for a very prolate trap. The longitudinal frequency $\omega_z = (2\kappa QV_{\rm EC}/m)^{1/2}$ is obtained from a dc potential $V_{\rm EC}$ applied to the eight end sections (end caps) of the electrodes, where $\kappa \approx 3 \times 10^{-3}$ mm^{-2} is a constant determined by the trap geometry.

For laser cooling of Be^+ ions we produce light resonant with the $^2S_{1/2}(F = 2) \rightarrow {}^2P_{3/2}$ transition at 313 nm by doubly resonant sum frequency generation, frequency stabilized to a hyperfine transition of molecular iodine [24]. The Be^+ fluorescence is simultaneously recorded with a photomultiplier and a CCD camera.

First, we load the trap with He^+ ions by leaking He gas into the vacuum chamber at a pressure of 10^{-8} mbar and ionizing it *in situ* by a 750 eV electron beam. The loading rate is controlled by the partial pressure of neutral He gas and the electron beam intensity. Subsequently, Be^+ ions are produced by ionizing neutral atoms evaporated from a Be oven with the same electron beam. During Be^+ loading the cooling and repumper lasers are continuously scanned over a 5 GHz interval below resonance.

One of the well-known signs for a phase transition from the fluid ion plasma to an ordered crystal state is the appearance of a sudden drop in the detected fluorescence attributed to the reduction in the particle velocities and thus Doppler broadening. Once this occurs, the cooling laser frequency is held constant at a red detuning of approximately half the natural linewidth (60 MHz) from the Be^+ resonance. Under this condition the crystals are stable, with a particle loss half time of $\sim$3 h.

Figure 1 shows three prolate two-component ion crystals containing Be^+ and He^+. The crystals display the well-known shell structure and enclose an inner dark region originating from the incorporated sympathetically cooled particles having a lower mass-to-charge ratio than that of the atomic coolants. Their location on axis is due to the stronger effective potential ($\sim Q^2/m$ for a strongly prolate trap, $\omega_r \gg \omega_z$) experienced by them as compared to the Be^+ ions. While Fig. 1(a) was taken with an axially symmetric potential, in Fig. 1(b) and 1(c) a static quadrupole potential $V_{\rm DC}$ was added The added potential turns the spheroidal crystal into an ellipsoid, squeezing the crystal in a direction at 45° to the observation direction [25]. This results in a redistribution of the ions such that fewer or no Be^+ ions remain in front and behind the He^+ ions. The shapes of large Coulomb crystals containing a small relative amount of He^+ ions agree well with the cold fluid plasma model [25,26].

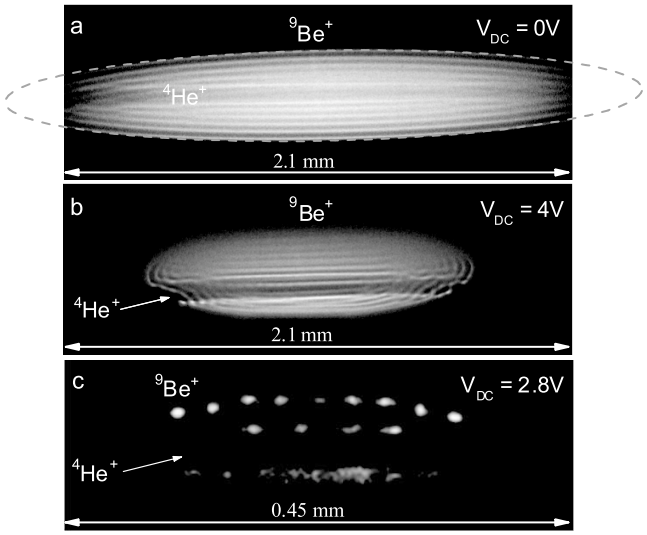

FIG. 1. CCD images of two-component Coulomb crystals (integration time: 2 s). (a) Spheroidal crystal. The ellipse is a fit to the crystal boundary with a semiaxes ratio $R/L = 0.16$. (b),(c) Ellipsoidal crystal. The inner dark cores contain $\approx$ 150, 30, and 5 sympathetically crystallized He^+ ions, respectively. The trap axis z is horizontal. For (a),(c) the cooling laser beam direction is to the right, for (b) two counterpropagating beams were used. The asymmetric ion distribution for (b),(c) is attributed to static stray potentials.

The number of crystallized particles is estimated by performing molecular dynamics (MD) simulations and varying the number of particles until the observed CCD image is reproduced. While for single-species structures one may obtain the particle number from the cold fluid model, which yields a particle density $n_0 = \epsilon_0 V_{\rm rf}^2/m\Omega^2 r_0^4$ ($\approx 3.1 \times 10^4$ mm^{-3} for Be^+), together with measured dimensions, here the MD approach is better suited. It is applicable to multispecies structures, in addition produces detailed structural information, and reduces uncertainties related to the calibration of the imaging system magnification. For example, MD simulations of the crystal in Fig. 1(a) show that it contains approximately 6.2×10^3 Be^+ ions and 150 He^+ ions. The radial intershell distance is obtained as 29 μm. This value agrees well with the

result calculated for infinite planar plasma crystals, $1.48(3/4\pi n_0)^{1/3} = 29.2\ \mu$m. According to the simulations, the He^+ ions are arranged in a zigzag configuration along the trap axis for two-thirds of the crystal, with a pitch spacing of $\approx 40\ \mu$m. In the remaining third (left end) the He^+ ions form a linear string, as evidenced by the smaller radial extension of the inner dark core. The asymmetric distribution is caused by light pressure forces on the Be^+ ions. Embedded strings were also observed in a mixed crystal of Ca^+ and Mg^+ ions where both ions were laser cooled [27].

An alternative way to roughly estimate the number of sympathetically cooled He^+ ions is as follows. Crystallized ions of any species are in force equilibrium at their locations $\mathbf{r}_i$. Thus, in a region occupied by a particular species, the space charge electric field takes on the values $Q\mathbf{E}(\mathbf{r}_i) = \nabla U_{\text{trap}}(\mathbf{r}_i)$. Consider now a closed smooth surface that is chosen such that it closely approaches many ion loci $\mathbf{r}_i$. We assume this relation approximately holds on the entire surface. Applying Gauss's law, the total charge Q_e enclosed by the surface is given by $Q_e = \epsilon_0 V_e \Delta U_{\text{trap}}/Q$, where V_e is the volume enclosed by the surface and a harmonic trap has been assumed, $\Delta U_{\text{trap}}(\mathbf{r}) = \text{const}$. The Laplacian also determines the constant charge density $\rho = \epsilon_0 \Delta U_{\text{trap}}/Q = n_0 Q$ of an ion species within the liquid charge model. Thus, the enclosed charge is simply the "displaced charge," $Q_e = \rho V_e$. We now apply this to the heavier particle species surrounding a cylindrical core containing lighter ions. Taking as the surface the cylinder bounded by the innermost Be^+ shell in Fig. 1(a) (radius $r_{\text{shell}} \simeq 35\ \mu$m) and extending to the ends of the dark core (length ≈ 2.2 mm), the estimate for the light species number is $N_{\text{He}} = Q_e/Q_{\text{He}} = Q_{\text{Be}} n_{0,\text{Be}} V_e/Q_{\text{He}} \simeq 260$. This is in reasonable agreement with the MD simulations, considering that the r_{shell} varies over the crystal length and the approximations made.

In order to identify the sympathetically cooled and crystallized ions we have performed mass spectroscopy by mass-selective excitation of transverse (secular) motion in the trap. A plate electrode was placed between two trap rods and an ac voltage applied. A secular scan is taken by varying the excitation frequency $\omega_{\text{ext}}/2\pi$ and recording the Be^+ fluorescence with the photomultiplier. The secular excitation pumps energy into the crystal; the resulting higher Be^+ ion velocities imply a line broadening. This leads to less fluorescence if the laser frequency lies near resonance, as is the case when the detuning is optimized for maximum cooling. Since the species are strongly coupled by Coulomb interaction, heating of one species will lead to energy transfer to the others.

Figure 2 shows images for a large two-component ion crystal before [2(a)] and after [2(c)] secular scans. Initially, the secular scan shows the presence of both Be^+ (283 kHz) and He^+ (685 kHz). The former value is close to the calculated value of 271 kHz. Regarding the He^+ resonance, we notice both an increase in fluorescence before resonance, and a substantial shift of the resonance peak from the theoretical value (613 kHz). We attribute this spread and shift to a modification of the secular frequency ω_r, which is a single-particle property, by the z dependence of the Be^+ ion distribution. The permanent increase of the fluorescence intensity before reaching the sharp He^+ secular excitation peak is due to partial removal of He^+ ions from the crystal by the high excitation amplitude.

After a few secular excitation cycles the He^+ ions were nearly completely removed from the trap, Fig. 2(c), leaving behind a nearly pure Be^+ ion crystal, as evidenced by the absence of secular resonance in Fig. 2(d). The small number of impurities remaining in the left end of the crystal did not lead to a fluorescence signal. Note that the visible crystal size has decreased substantially because of Be^+ ion loss. Nevertheless, the absolute fluorescence intensity of the final Be^+ crystal is essentially equal to the level at the end of the first secular scan. This may be explained by a lower ion temperature or reduced micromotion. Moreover,

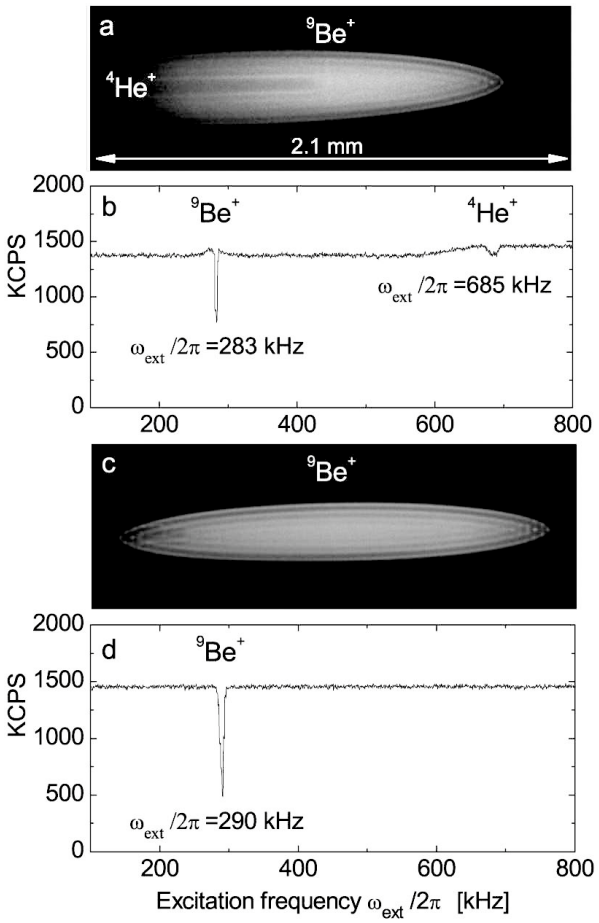

FIG. 2. (a) Prolate two-component Coulomb crystal (cooling laser beam direction to the right). (b) Corresponding Be^+ fluorescence signal vs secular excitation frequency $\omega_{\text{ext}}/2\pi$. (c) Ion crystal after removal of He^+ through repeated secular excitation. (d) Corresponding secular excitation spectrum. Time between (a),(b) and (c),(d): 5 min. Frequency scans are toward increasing frequency.

a shift of the crystal with respect to the trap occurred in the direction of the propagation of the laser beam. We attribute this to stronger light pressure forces experienced by the Be^+ ions, which is consistent with the increased fluorescence level per ion.

A central question concerning sympathetically cooled ions is their translational temperature; several observations can shed light on the answer. A direct measurement on $^{24}Mg^+$ embedded in a laser-cooled $^{40}Ca^+$ crystal yielded an upper limit of 45 mK, deduced from the $^{24}Mg^+$ laser excitation linewidth [20]. In a two-ion crystal sympathetic cooling to the Doppler limit (<1 mK) has been shown [23]. MD simulations for small particle numbers have shown that sympathetic ions caged by laser-cooled ions are essentially in thermal equilibrium with the latter at the Doppler temperature [22]. Thus, an estimate of the sympathetic temperature may be obtained from the temperature of the laser-cooled ions. We deduce a direct upper limit for the translational temperature of the Be^+ from the spectral line shape of their fluorescence as the cooling laser is tuned towards resonance and the ion ensemble crystallizes. We fit an appropriate Voigt profile to each point of the recorded fluorescence curve to determine the Be^+ temperature. For small crystals (<1000 particles), we find an upper limit at the end of the scan of 42 mK. An indirect upper limit is obtained by comparing the size of the ion spots with MD simulations; here we find a tighter limit of <20 mK for the Be^+ temperature. We therefore deduce, assuming thermal equilibrium, that the He^+ temperature is <20 mK.

In summary, we have sympathetically cooled and crystallized He^+ ions using laser-cooled Be^+ ions in a linear Paul trap. Large Coulomb crystals of $\sim 6.2 \times 10^3$ Be^+ ions contained about 150 He^+ ions, arranged in a zigzag structure centered on the trap axis. The mass ratio of 0.44 between sympathetically cooled and laser-cooled ions is the lowest achieved so far for large ion ensembles in a Paul trap. We estimate the temperature of the crystallized He^+ ions at below 20 mK.

Translationally cold and immobilized He^+ ions are a promising system for high precision spectroscopy and might lead to more precise atomic and nuclear constants. The weak $1S$-$2S$ transition in He^+ could be detected with a high signal to noise ratio using a single adjacent Be^+ ion as a ''quantum sensor,'' rather than by direct detection of its fluorescence [28]. Significant progress in this direction has been achieved [23,29]. Moreover, sympathetically cooled He^+ opens up perspectives for studies of cold collisions and cold chemistry, e.g., generation of $^3HeH^+$ molecules, whose hyperfine structure is of interest in fundamental physics [30].

The $^4He^+/^9Be^+$ cooling and crystallization results also have implications for the possibility of achieving this with highly charged atomic ions (HCAI). Favorably, the q parameters are similar and the effective potential is steeper for the HCAIs than for the $^9Be^+$. Under appropriate conditions, the laser-cooled $^9Be^+$ ions are expected to cage the HCAIs, leading to efficient cooling.

We thank the Deutsche Forschungsgemeinschaft (DFG) and the EU network HPRN-CT-2002-00290 for support. We are grateful to D. Leibfried for helpful suggestions, H. Wenz for the MD simulations, and S. Karshenboim for discussions.

Note added.—We have also produced two-species Coulomb crystals containing $^3He^+$ reliably.

[1] See, e.g., *Precision Physics of Simple Atomic Systems*, edited by S. G. Karshenboim *et al.* (Springer, New York, 2001); M. I. Eides *et al.*, Phys. Rep. **342**, 63 (2001).
[2] J. D. Gillaspy, J. Phys. B **34**, R93 (2001).
[3] See, e.g., V. M. Shabaev *et al.*, Phys. Rev. Lett. **86**, 3959 (2001), and references therein.
[4] J. Verdu *et al.*, Phys. Rev. Lett. **92**, 093002 (2004).
[5] B. de Beauvoir *et al.*, Eur. Phys. J. D **12**, 61 (2000).
[6] H. A. Schuessler *et al.*, Phys. Rev. **187**, 5 (1969); M. H. Prior and E. C. Wang, Phys. Rev. A **16**, 6 (1977); for the theory, see S. G. Karshenboim and V. G. Ivanov, Eur. Phys. J. D **19**, 13 (2002).
[7] A. van Wijngaarden *et al.*, Phys. Rev. A **63**, 012505 (2000).
[8] U. D. Jentschura and G. W. F. Drake, Can. J. Phys. **82**, 103 (2004).
[9] D. Shiner *et al.*, Phys. Rev. Lett. **74**, 3553 (1995).
[10] J. L. Flowers *et al.*, NPL Report No. CBTLM 11 (2001); T. W. Hänsch (private communication).
[11] S. A. Burrows *et al.*, in *Laser Spectroscopy*, edited by R. Blatt *et al.* (World Scientific, River Edge, NJ, 1999), Vol. 14.
[12] QED uncertainty without nuclear radius effect $\sim 6 \times 10^4$ Hz, nuclear radius effect uncertainty $\sim 7 \times 10^4$ Hz [1,8], uncertainty due to Rydberg constant $\sim 8 \times 10^4$ Hz. For the $2S$-$3S$ transition, the situation is somewhat less favorable due to a larger relative contribution of the R_∞ uncertainty and the larger transition linewidth.
[13] See, e.g., *Proceedings of the 6th Symposium on Frequency Standards and Metrology*, edited by P. Gill (World Scientific, River Edge, NJ, 2002).
[14] F. G. Major and H. G. Dehmelt, Phys. Rev. **170**, 91 (1968).
[15] R. Drullinger *et al.*, Appl. Phys. **22**, 365 (1980).
[16] D. Larson *et al.*, Phys. Rev. Lett. **57**, 70 (1986).
[17] M. Raizen *et al.*, Phys. Rev. A **45**, 6493 (1992).
[18] I. Waki *et al.*, Phys. Rev. Lett. **68**, 2007 (1992).
[19] P. Bowe *et al.*, Phys. Rev. Lett. **82**, 2071 (1999).
[20] L. Hornekær, Ph.D. thesis, Aarhus University, 2000.
[21] T. Harmon *et al.*, Phys. Rev. A **67**, 013415 (2003).
[22] S. Schiller and C. Lämmerzahl, Phys. Rev. A **68**, 053406 (2003).
[23] M. D. Barrett *et al.*, Phys. Rev. A **68**, 042302 (2003).
[24] H. Schnitzler *et al.*, Appl. Opt. **41**, 7000 (2002).
[25] U. Fröhlich *et al.* (to be published).
[26] L. Turner, Phys. Fluids **30**, 3196 (1987).
[27] L. Hornekær *et al.*, Phys. Rev. Lett. **86**, 1994 (2001).
[28] D. J. Wineland *et al.*, in Ref. [13], pp. 361–368.
[29] B. B. Blinov *et al.*, Phys. Rev. A **65**, 040304(R) (2002).
[30] S. G. Karshenboim (private communication).